Name_____Student ID_____Section_____

Prince of Songkla University

Faculty of Engineering

Department of Computer Engineering

Midterm Examination: Semester 2 Acadimic Year: 2011

Date: 22 December 2011 Duration: 09:00-12:00

Subject: 241-500 Research and Development Methodologies Room: R200

Nikom SUVONVORN, PhD.

- There are 4 parts, 7 pages for 100 marks. Answer all questions.
- Calculator, books, documents, and writing stationery are **not allowed**.
- Dictionary **is allowed**.
- Write an answer on this examination paper. If there is not enough space, use the back page.
- Write your name and student code on all pages.

Name: ..... Student ID:.....

Corruption in the exam:

The minimum penalty is to invalidate this course and suspend your study for one semester.

Name_____Student ID_____Section_____

1. Draw a diagram of the research process, and explain each step in detail.

Name_____Student ID_____Section_____

2. Extract the following issues from the first research work **(paper no.1)**.

2.1 Research problem

2.2 Hypostasis

2.3 Independence and dependence variables

2.4 Keywords

Name_____ Student ID_____ Section_____

2.5 Explain the proposed methods (in brief)

2.6 Conclude on the identified variables.

2.7 What should be the title of this paper?

Name_____ Student ID_____ Section_____

3. Extract the following issues from second research work **(paper no.2)**

3.1 Research problem

3.2 Hypostasis

3.3 Independence and dependence variables

3.4 Keywords

3.5 Explain the proposed methods (in brief)

3.6 Conclude on the identified variables.

3.7 What should be the title of this paper?

Name_____Student ID_____Section_____

4. Please introduce ideas for establishing a novel research topic on oil palm grading by applying the techniques proposed by paper no.1 and no.2. Define the following key issues: problem, hypothesis, variables, title, and keywords.

ABSTRACT

In this paper, a computer vision based system is introduced to automatically grade apple fruits. Segmentation of defected skin is done by three global thresholding techniques (Otsu, isodata and entropy). Stem-end/calyx regions falsely classified as defect are removed. Segmentations were visually best with isodata technique applied on 750nm filter image. Statistical features are extracted from the segmented areas and then fruit is graded by a supervised classifier. Linear discriminant, nearest neighbor, fuzzy nearest neighbor, adaboost and support vector machines classifiers are tested for fruit grading, where the latter outperformed others with 89 % recognition.

1. INTRODUCTION

Computer vision based quality sorting of apple fruits is a hard but necessary task for increasing the speed of sorting as well as eliminating the human error in the process. Segmentation of skin defects of apples is one of the major problems of this field where research still continues to accurately segment and identify these defects. In order to segment defects Leemans et al. introduced a Gaussian model of skin color for 'Golden Delicious' [1], and a Bayesian classification method for 'Jonagold' apples [2], where healthy skin presenting patches was segmented as defected in the former and segmentation of russet defects and color transition areas of skin were problematic in the latter. Rennick et al. used a controlled acquisition system and different classifiers to classify skin color and detect blemishes of 'Granny Smith' apples [3]. Yang introduced an automatic system to detect patch-like defects on apples, where he used flooding algorithm to segment defects, structural light and neural networks to find stem-ends and calyxes and snakes algorithm to refine defected areas [4]. Unay and Gosselin introduced a neural network based system to segment defects on 'Jonagold' apples, where segmentation was accurate, but misclassification of stem-end, calyx areas as defects occured [5].

2. METHODS

2.1 Image Acquisition and Database

Database consists of one-view images of 'Jonagold' apples taken from diffusely illuminated environment by a high resolution monochrome digital camera with four interference band-pass filters centered at 450nm (BL), 500nm (GR), 750nm (RE), and 800nm (IR) with respective bandwidths of 80, 40, 80, and 50 nm. Each filter image is composed of 430x560 pixels with 8 bits-per-pixel resolution (Figure 1). 280 of the fruits were healthy whereas 246 of them included several skin defects (russet, recent bruises, rot, scald, hail damage, scar tissue, limb rubs,...) in varying size and shapes. 'Jonagold' variety is selected, instead of mono-colored ones, because it has a bi-colored skin causing more difficulties in segmentation due to color transition areas. Some RGB images of the database can be observed in Figure 2.

Image acquisition and database collection of this work are done in Mechanics and Construction Department of Gembloux Agricultural University of Belgium, and related details can be found in the works of Kleynen et al. [6], [7].

Figure 1: Filter images of a fruit. Left to right: BL, GR, RE, and IR filters.

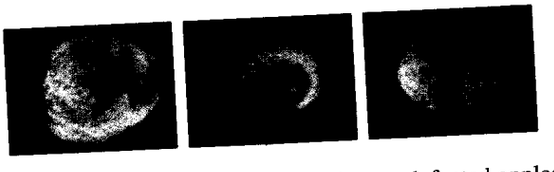

Figure 2: Original (RGB) images of some defected apples.

2.2 Pre-Processing

The database is composed of images of apple views on a dark, uniform colored (i.e. low intensity) background. Therefore, fruit area can be separated from background by thresholding the RE filter image at intensity value of $\approx$ 11,77 %. Our visual observations have shown that fixed thresholding can remove low intensity regions like some defects, stem-ends or calyxes. Hence, a morphological filling operation is also applied to remove these holes.

Our initial observations revealed that segmentation was problematic at the far edges of fruit probably due to illumination artifacts. Therefore, after background removal, fruit area is eroded by a rectangular structuring element with size adaptive to fruit size. Dimensions of the structuring element are calculated as 15 % of the horizontal (a) and vertical (b) dimensions of fruit bounding-box.

2.3 Defect Segmentation

Thresholding can be applied locally, i.e. within a neighborhood of each pixel, or globally. Due to highly varying defect

sizes, it will be impossible to find one neighborhood size that works for all. Thus, following global thresholding techniques are tested for defect segmentation in this work:

- *Otsu* : Otsu's method is still among the most referenced methods in segmentation [8]. It is based on minimizing within-class variances of foreground and background pixels.
- *Entropy* : Kapur et al. explained foreground and background of an image as different signals [9]. Therefore, optimal threshold is the one maximizing the sum of the two class entropies (Eq. 1).

$$H = max\Big[-\sum_{i=0}^{T_{opt}} p_i log(p_i) - \sum_{i=T_{opt}+1}^{255} p_i log(p_i)\Big] \quad (1)$$

- *Isodata* : Ridler and Calvard assumed image as a two-class Gaussian mixture model and proposed an iterative technique, which calculates a new threshold by averaging the foreground and background class means at each iteration [10]. If change in thresholds between two consecutive iterations is small enough (0.04 %), then algorithm stops.

Above thresholding techniques are applicable on gray-level (2-dimensional) images. However in a multi-spectral imaging system, one can either combine the filter images to get a final gray-level image or select one of the filter images by a criterion. As the optimal combination is arduous, in this work we consider using filter images separately and try to select the optimum pair of filter image and thresholding technique.

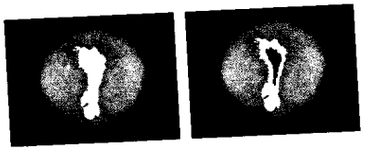

Figure 3: Example of stem-end/calyx removal. Before the removal on the left, and stem-end/calyx removed on the right. Defected area displayed in white in both images.

Stem-end and calyx, which are natural parts of apple fruit, appear as dark blobs on the images like some of the true defects. But, threshold-based segmentation does not consider presence-absence of these regions, while partitioning fruit area into defected and healthy parts. Thus, segmentation should be refined to remove stem-end/calyx.

Stem-end/calyx recognition method, which was previously introduced by the authors [11] and found to be highly accurate, is used in this work. It starts with background removal and threshold-based object segmentation. Then, statistical, textural and shape features are extracted from each segmented object and these features are introduced to support vector machines classifier, which discriminates true recognitions from false ones. So, the regions identified as stem-end/calyx by this method are removed from the formerly detected segmentation result. Figure 3 displays an example of such a refinement step, which demonstrates the improvement in the defect segmentation.

2.4 Feature Extraction

Main goal of our project is to provide a fast algorithm for fruit classification. Therefore, *average*, *standard deviation*, and *median* values are calculated over the segmented area of each fruit from all filter images. In addition to these 12 features, *defected ratio*, which is the ratio of defected pixels of the fruit, is also computed. Thus, each fruit is represented by 13 features, which are normalized to have an average of zero and standard deviation of one before the classification step.

2.5 Fruit Classification

The following supervised classifiers are tested in this paper.

- *Linear Discriminant Classifier* (LDC) searches for a linear decision boundary that separates the feature space into two half-spaces by minimizing the criterion function

$$g(x) = w^t x + w_0 \quad (2)$$

- *Nearest Neighbor Classifier* (k-NN) assigns an object to the most represented category among the k (5) nearest samples of that object. Similarity measure used to find nearest samples is the Euclidean distance.
- *Fuzzy Nearest Neighbor Classifier* (fuzzy k-NN) is the fuzzified version of k-NN. Fuzziness is acquired using the distance information of k (5) nearest neighbors to the new sample by,

$$u_i(x) = \frac{\sum_{j=1}^{k} u_{ij}\left(\|x - x_j\|\right)^{\frac{-2}{m-1}}}{\sum_{j=1}^{k}\left(\|x - x_j\|\right)^{\frac{-2}{m-1}}} \quad (3)$$

$u_i(x)$ is the predicted membership value of test sample x for class i, u_{ij} is the membership (either 0 or 1) of j^{th} neighbor to the i^{th} class and m is the *fuzzifier* parameter (set to 2) that determines how heavily the distance is weighted.

- *Adaptive Boosting* (AdaBoost) tries to form a final strong classifier (g) from an ensemble of weak learners (h_t) by continuously adding these weak learners until the desired training error is reached [12]. Thus, decision for a test sample x is taken by:

$$g(x) = sgn\Big[\sum_{t=1}^{t_{max}} \alpha_t h_t(x)\Big] \quad (4)$$

where α_t are the coefficients found by boosting process, t_{max} is the number of weak learners and *sgn* returns the sign of the value.

- *Support Vector Machines* (SVM) is a statistical learning method based on structural risk minimization [13]. In the binary case, SVM tries to find the hyperplane that separates the classes with maximum *margin* by non-linear mapping. For a test sample x, classification is done by:

$$y = sgn\Big(\sum_{i=1}^{N} \alpha_i y_i K(s_i, x)\Big) \quad (5)$$

$$K(s_i, x) = e^{-\frac{\|s_i - x\|^2}{2\sigma^2}} \quad (6)$$

where N is the number of training samples, y_i is the class label, $K(s_i, x)$ is the kernel function and α_i is the Lagrangian multiplier bound by $0 \leq \alpha_i \leq C$. x_i's for which

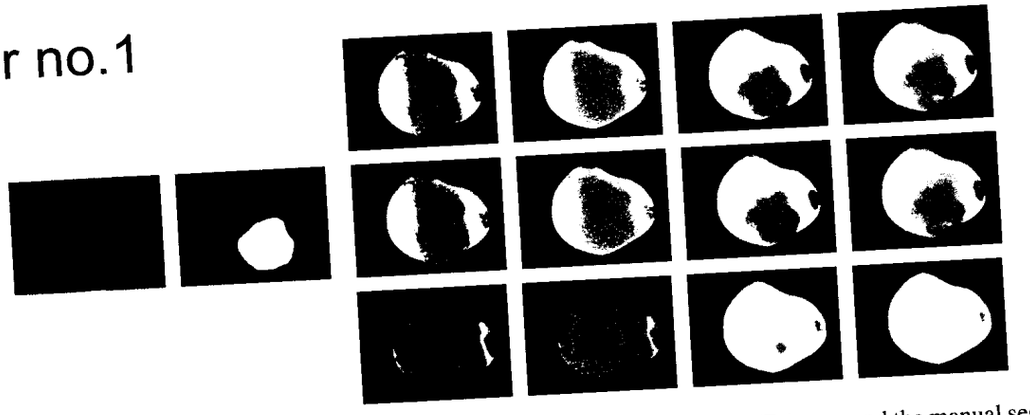

Figure 4: Segmentation results of thresholding methods on a bruised apple. Original RGB image and the manual segmentation (ground truth) of the fruit are on the left. Subsequent synthetic images show defected regions in gray and healthy ones in white. Each row belongs to a thresholding method (top-to-bottom: otsu, isodata, entropy) and each column shows a band (left-to-right: BL, GR, RE, IR).

$\alpha_i > 0$ are called the support vectors. Gaussian radial basis function kernel (Eq. 6) and $C = \infty$ are chosen for this work.

Evaluation of the classification process is measured by K-fold cross-validation method, with K=5. Furthermore, samples of the dataset are randomly ordered before being introduced to the classifier, to prevent biased classification for sample order.

In this research, libraries of Almeida [14] and Räetsch [12] are used for SVM and AdaBoost classifications, respectively. The proposed system is implemented under Matlab 6 R12.1 environment [15].

3. RESULTS AND DISCUSSION

Defect segmentation results of a bruised fruit using thresholding techniques on filter images are displayed in Figure 4. Bruise is selected for display, because it is one of the most common defects of apple fruits. As an initial observation, in the results of BL and GR filter images, false segmentations are observed. This is probably because in these filter images (i.e. in the wavelength range of [410-510] nm) contrast between healthy skin and the defect is low. Within the results of RE and IR filter images, those of entropy technique are visually unacceptable; almost no part of defect is found. On the other hand, otsu and isodata techniques provide satisfactory results, favorably on RE filter image. Although results of bruise type of defect are discussed here only, above observations are mostly consistent within the database, i.e. our visual examinations on the results of all images of the database confirm that isodata technique should be applied on RE filter image for the best output.

Figure 5 provides more segmentation results of fruits with different defects produced by isodata technique on RE and IR filter images. Scald (top-left) and hail damage perfusion (bottom-left) defects are partially segmented in both filter images. Segmentation of frost damage (mid-left) and rot (top-right) defects are acceptable for RE, whereas results of IR are under-segmented. Finally, for bruise (mid-right) and flesh damage (bottom-right) defects none of the segmentations are satisfactory. In general, results of RE filter image are visually better than those of IR. Results displayed here are before the SC removal step, therefore some stem-end regions are observed as defect, which are corrected later on.

Following segmentation, SC removal and feature extraction steps, fruits are graded as healthy or defected by different supervised classifiers, performances of which are observed in Table 1. As we go from simple to sophisticated classifiers, recognitions increase. LDC (simple) performs around 79 % and nearest neighbor classifiers (more sophisticated) around 83 %, whereas AdaBoost and SVM (most sophisticated) reach to 88-89 % rates. Fuzziness does not have significant impact on recognition. Especially in the results of AdaBoost and SVM, superiority of isodata method and RE filter image are obvious, which is consistent with our visual observations. Highest recognition rate is observed by SVM classifier on isodata method and RE filter image with 89.2 %.

4. CONCLUSION

In this article a computer vision based automatic sorting system for apple fruits is introduced. The fruit area is extracted from the background and it is eroded to reduce undesired effects of illumination. Then, defected areas of fruit are segmented by three global thresholding methods applied on filter images separately. Visual results showed that segmentation accuracy was better on RE and IR filter images. Furthermore, isodata thresholding method was found to outperform others. As stem-end or calyx regions also appear as defects in the segmentation, these parts are removed by a method previously introduced by the authors. Finally, statistical features are extracted from segmented defects and fed to several supervised classifiers for fruit grading by binary classification (defected or healthy). Highest recognition rate is observed by support vector machines classifier with 89.2 %. Observations on the performances of classifiers not only confirmed superiority of isodata method and RE filter image, but also revealed that more sophisticated classifiers lead to better recognition rates.

5. ACKNOWLEDGEMENT

This research is funded by the General Directorate of Technology, Research and Energy of the Walloon Region of Belgium with Convention No 9813783. We would also like to

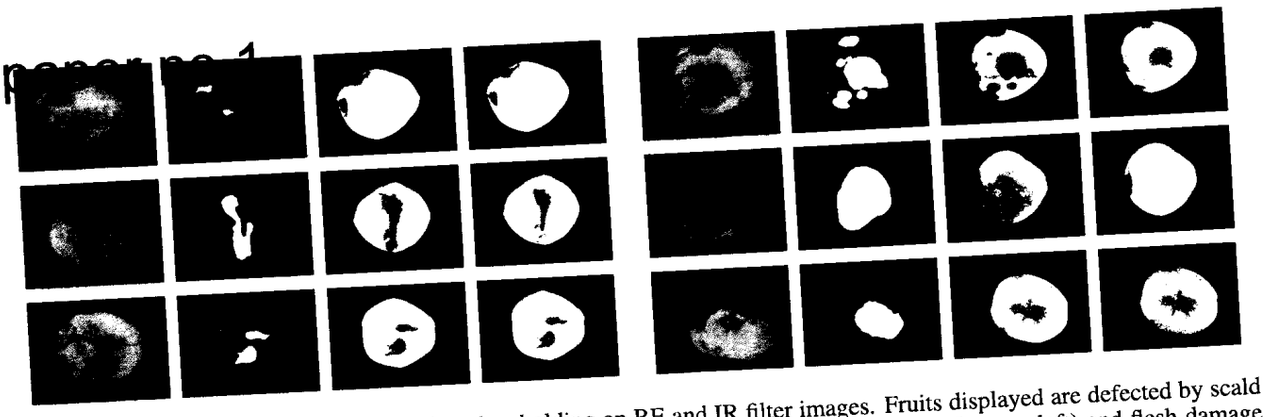

Figure 5: Results of segmentation by isodata thresholding on RE and IR filter images. Fruits displayed are defected by scald (top-left), rot (top-right), frost damage (mid-left), bruise (mid-right), hail damage perfusion (bottom-left) and flesh damage (bottom-right). For each fruit its original RGB image, its manual segmentation (ground truth) and its segmentation results (from RE filter image on the left and from IR on the right) are displayed in a row. Defected areas are displayed in white in ground truth images, whereas segmentations show defected regions in gray color and healthy ones in white.

band	method	LDC	5-NN	Fuzzy 5-NN	AdaBoost	SVM
RE	otsu	81.8	84.4	83.8	87.5	87.8
	isodata	78.5	83.5	83.5	88.4	**89.2**
	entropy	78.0	79.1	79.5	84.5	83.8
IR	otsu	78.9	82.9	83.5	86.3	86.0
	isodata	75.7	81.6	82.1	88.2	87.6
	entropy	78.9	78.0	78.3	82.9	81.9

Table 1: Classification performances of classifiers in correct recognition percentages.

thank Prof. M.-F. Destain, O. Kleynen and V. Leemans from Gembloux Agricultural University of Belgium for providing the image database.

REFERENCES

[1] V. Leemans, H. Magein, and M.-F. Destain. Defect segmentation on 'golden delicious' apples by using colour machine vision. *Computers and Electronics in Agriculture*, 20(2):117–130, July 1998.

[2] V. Leemans, H. Magein, and M.-F. Destain. Defect segmentation on 'jonagold' apples using colour vision and a bayesian classification method. *Computers and Electronics in Agriculture*, 23(1):43–53, June 1999.

[3] G. Rennick, Y. Attikiouzel, and A. Zaknich. Machine grading and blemish detection in apples. In *Proc. 5th Int. Symp. Signal Processing and Appl.*, pages 567–570, Brisbane, Australia, August 1999.

[4] Q. Yang. Automatic detection of patch-like defects on apples. In *Proc. 5th Image Processing and Its Appl.*, pages 529–533, Edinburgh, UK, July 1995.

[5] D. Unay and B. Gosselin. A quality sorting method for 'jonagold' apples. In *Proc. Int. Agricultural Engineering Conf. (AgEng)*, Leuven, Belgium, September 2004.

[6] O. Kleynen, V. Leemans, and M.-F. Destain. Selection of the most efficient wavelength bands for 'jonagold' apple sorting. *Postharvest Biology and Technology*, 30(3):221–232, December 2003.

[7] O. Kleynen, V. Leemans, and M.-F. Destain. Development of a multi-spectral vision system for the detection of defects on apples. *Journal of Food Engineering*, page in press, 2004.

[8] N. Otsu. A threshold selection method from gray-level histograms. *IEEE Transactions on Systems, Man and Cybernetics*, 9(1):62–66, 1979.

[9] J.N. Kapur, P.K. Sahoo, and A.K.C. Wong. A new method for gray-level picture thresholding using the entropy of the histogram. *Graphical Models and Image Processing*, 29:273–285, 1985.

[10] T.W. Ridler and S. Calvard. Picture thresholding using an iterative selection method. *IEEE Transactions on Systems, Man and Cybernetics*, SMC-8:630–632, 1978.

[11] D. Unay and B. Gosselin. A stem-end/calyx recognition system based on pattern recognition for 'jonagold' apples. Technical report, TCTS Labs., Faculté Polytechnique de Mons, 2004. available upon request.

[12] G. Rätsch, T. Onoda, and K.-R. Müller. Soft margins for AdaBoost. *Machine Learning*, 2000.

[13] C.J.C. Burges. A tutorial on support vector machines for pattern recognition. *Data Mining and Knowledge Discovery*, 2:121–127, 1998.

[14] M.B. Almeida, A.P. Braga, and J.P. Braga. Svm-km:speeding svm's learning with a priori cluster selection and k-means. In *Proc. 6th Brazilian Symposium on Neural Networks*, pages 162–167, Rio de Janeiro, Brazil, January 2000.

[15] MathWorks Inc. Matlab: The language of technical computing, http://www.mathworks.com, 1984-.

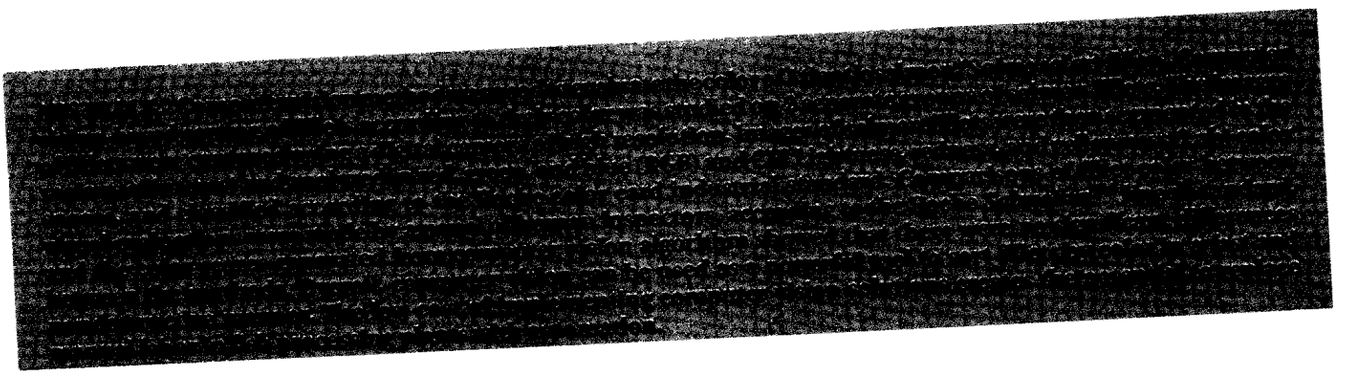

Introduction

During the last few decades, the number of whitefish processing plants in Norway has diminished considerably for several reasons. In aquaculture, although the production volume of salmonids has increased tremendously over the same period of time, most fish are exported as raw material, that is, gutted fresh or frozen fish. In both sectors, fish processing is often unprofitable due to the high labor costs. For instance, where salmonids are filleted, the manpower needed on the filleting line alone is typically 20 to 40 persons per shift to process 35 tons of bled, gutted fish from the slaughter line. Ostvik and Jansson (2004) reported that Norway with the present technological level has the highest production cost in fisheries compared to Poland and China. Labor costs represent the bulk of the production costs in Norway. They estimate that the automation of fish processing plants employing computer vision and other robotic machinery in substituting human inspectors would bring savings in labor costs of approximately $1 per produced kilogram of fish.

One of the operations along the fish processing line is color grading of salmon fillets. It is generally accepted that color of salmon products is one of the most important quality parameters in fish processing. Consumers associate redder salmon with being fresher, having better flavor, higher quality, and higher price (Anderson 2000). In addition, different markets tend to have special preferences concerning fillet color. According to market analysis from SalmoBreed (Osland 2001), the Japanese market, for instance, prefers fillets with a deeply red color.

According to the Norwegian Standard NS 9402 (1994), the color measurement of salmon fillets is done using the Roche color cards. Human inspectors are trained to grade fillets by color according to these cards. This manual grading has several drawbacks. First, it greatly increases the production costs. Second, the color grading is not fast, and it is not consistent because human inspectors are subjected to factors such as eye fatigue, lack of color memory, and variations in color discrimination (Irudayaraj and Gunasekaran 2001), resulting in mistakes and occasional omissions in processing. These factors may decrease the product quality and thereby reduce profit (Pau and Olafsson 1991).

Automation of fish processing with computer vision, apart from savings in labor costs, can bring also an overall improvement in the product quality (Arnarson and others 1988). In food industry, there has been a rapid growth over the past decade in development and use of noninvasive methods to evaluate quality (Lin and others 2003). Although a huge variety of examples of using computer vision in food industry have been reported (Panigrahi and Gunasekaran 2001), the use of computer vision in automation of fish processing industry is still limited.

A typical computer vision system (Figure 1) consists of the illumination setup for the acquisition of scene images, a camera for image capturing, and a PC. After the images are captured, they are sent to the computer for further processing. The computer is used for designing the algorithm that enables feature extraction, segmentation, quantification and classification of images, and the objects of interest contained in these images. Feature extraction consists of the choice of distinguishing features that can be used for discriminating patterns in different categories (Duda and others 2001). Segmentation is used to subdivide the image into its constituent regions of interest (Gonzales and others 2004). Two steps are important in the computer vision algorithm design stage: image processing and image analysis. Image processing involves a series of image operations that enhance the quality of image in order to remove defects such as geometric distortion, noise, and nonuniform lighting. Image analysis is the process of distinguishing the objects (regions of interest) from the background and giving quantitative information used for decision making (Brosnan and Sun 2004). Computer vision has

MS 20060272 Submitted 5/12/2006, Accepted 11/9/2006. Authors Misimi, Mathiassen, and Erikson are with SINTEF Fisheries and Aquaculture, N-7465 Trondheim, Norway. Author Misimi is with Dept. of Engineering Cybernetics, NTNU, N-7491 Trondheim, Norway. Direct inquiries to author Misimi (E-mail: ekrem.misimi@sintef.no).

paper no.2

doi: 10.1111/j.1750-3841.2006.00241.x

proven successful for online process control and inspection of food and agricultural products with applications ranging from simple automatic visual inspection to more complex vision control (Panigrahi and Gunasekaran 2001). Mery and Pedreschi (2004) used computer vision for segmentation of color fruit images. Abdullah and others (2000) examine the color of muffins with a computer vision system for separating dark from light samples using pregraded and nongraded muffins. Davidson and others (2001) showed how digital images could be used to estimate physical features such as the color of baked dough. Brosnan and Sun (2004) presented a review on how computer vision can be used to estimate the quality in certain foods such as bakery products, meat, fish, vegetables, grains, fruits, and so on. In fish processing, Strachan and Murray (1991) present a machine, which is based on computer vision, for sex discrimination of mature herring. Misimi and others (2006) have used the computer vision to classify Atlantic salmon in 2 grading classes. Here, a computer vision algorithm was designed to extract the geometrical features of salmon: length, width, area, and ratios among these. Having generated this set of features, a classifier was designed and trained to be able to grade salmon into 2 grading classes: "production grade" with many external deformities and "superior grade" without visible external flaws.

The idea of using color for in-cannery sorting of raw salmon was tested by Schmidt and Cuthbert (1969). They reported that reflectometer measurements using the ratio 650:570 nm correlated well with visual assessment and Hunter a and b value assessments of flesh color. Color in computer vision has also been used as sorting criteria for classification of fish species (Strachan 1993).

Our goal was to show that, by using computer vision, color of fillets could be quickly assessed from a single image. As a rule of thumb, any method should be able to perform such assessments at about 1 s or less per fillet to cope with the speed of the production line. This restriction alone as well as the contact free feature of computer vision in "evaluating quality excludes a number of other sensors that may otherwise be suitable. In the present study, we wanted to compare our computer vision results with the values determined manually using the Roche *Salmo*Fan™ lineal ruler and Roche color card, which according to standard NS 9402 (1994) are used for evaluation of color of salmonids by the fish processing industry.

Materials and Methods

Fish and fish sampling

Atlantic salmon (*Salmo salar*) from 2 different fish processing plants (Marine Harvest and Salmar AS, Hitra, Norway) was used.

Group I: Four "Superior Grade" (weight: 3.7 ± 0.4 kg, length: 60 ± 3 cm, condition factor range: 1.50 to 1.84) and 1 sexually mature fish (weight: 4.3 kg, length: 71 cm, condition factor: 1.19) were selected from the slaughter line on November 12, 2004, at the Marine Harvest salmon processing plant. According to the Norwegian Industry Standard for Fish NBS 10-01 (1999), a "Superior Grade" salmon is a first class product without substantial faults, damage, or defects, and provides a positive overall impression. Condition factor (K) is a number that is used to quantify the condition of fish. Fulton (1902) proposed to use a mathematical formula for this quantification:

$$K = \frac{10^5 W}{L^3} \quad (1)$$

where W is the weight of the fish in grams (g), L is the length of fish in millimeters (mm).

Fish with the condition factor $K = 1$ are considered as poor fish (Barnham and Baxter 1998) because they are long and thin. Fish with $K = 1.4$ are considered to be good fish, being well proportioned, while fish with condition factor $K = 1.6$ are fish in excellent condition.

The fish, except the sexually mature fish, were bled and gutted at the plant. All fish were transported to our laboratory in styrofoam boxes containing ice. The fish were subjected to postrigor analysis 3 d postmortem. The core temperature was 1.4 ± 0.4 °C. At this point, the sexually mature fish was filleted. Fillet color ($n = 8$) was determined using sensory evaluation, a Minolta chromameter, and a computer vision system.

Group II: "Superior Grade" fish (weight: 5.6 kg ± 1.0 kg, length: 74 cm ± 5 cm, mean condition factor: 1.4, $n = 18$) were sampled individually (January 5, 2005) from a commercial processing line (Salmar AS) prior to killing and further processing (that is, the fish were not bled). Our fish were rapidly killed by a blow to the head, placed in styrofoam boxes containing ice, and transported to our laboratory. Fish were stored on ice in a cold room at 5 °C. The fish had been fasted for 30 d before slaughter and the content of astaxanthin in the muscle of fish from the same batch (cage) was 7.3 mg/kg. After 4 d of ice storage, the fish were filleted (postrigor) before being subjected to the various analyses the same day. The ultimate fillet pH was 6.46 ± 0.06 ($n = 18$). The fillets were of very good quality, with a firm, elastic texture with practically no visual signs of gaping. The following fillet quality-related parameter was assessed: color ($n = 33$). The assessment was done using the sensory evaluation method, the Minolta chromameter, and the computer vision system.

Sensory evaluation of color

The color of the fillets (both groups) was descriptively evaluated by 3 panelists according to the Norwegian Standard NS 9402 (1994) for measuring color of Atlantic salmon. This evaluation was performed visually in the daylight using Roche color cards (Figure 3.)

Instrumental evaluation of color

L^*, a^*, and b^* values (CIE 1976) were measured using a Minolta Chromameter CR-200/CR231 (Minolta, Osaka, Japan). Color readings for all fillets were taken at the same day when the sensory

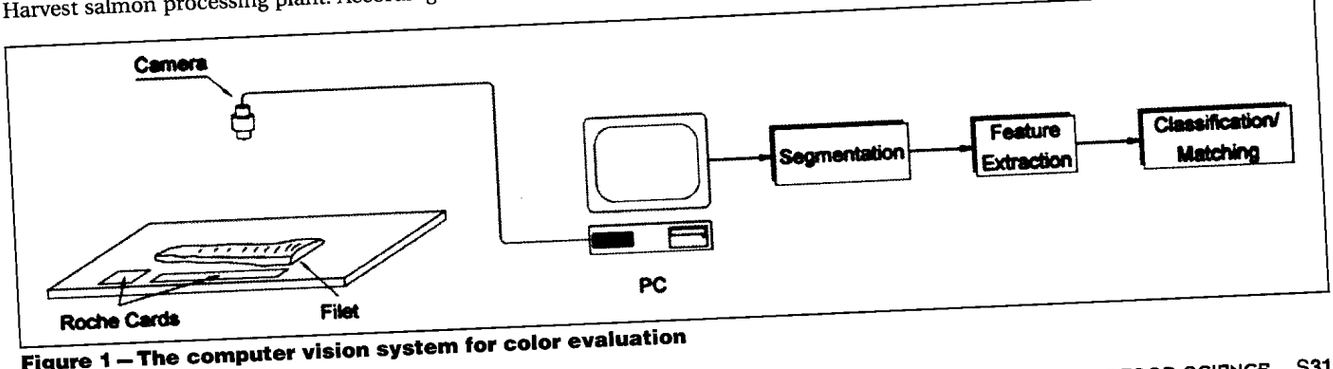

Figure 1 – The computer vision system for color evaluation

evaluation of color of fillets was performed and prior to taking the image with digital camera. The chromameter consists of a pulsed xenon lamp that illuminates the surface of the fillet and collects the reflected light for color analysis. For all fillets of both groups, the color-related assessments were carried out in white muscle (locations 1 to 3) and in the belly flap (locations 4 to 5) (Figure 2). Here, L^* denotes lightness in the scale of 0 to 100 from black to white, a^* is redness (+) values are red whereas (–) values denote green and b^* denotes yellowness (+)–yellow or (–)–blue. The chromameter instrument was calibrated using a standard white plate and was positioned perpendicular to the fillet surface when the measurements were taken. The chromameter measurements were collected over the 8 mm dia of the probe area.

Computer vision evaluation of color

Each fillet from both groups was photographed (Figure 2) along the Roche *Salmo*Fan ruler (range: 20 [pink] to 34 [dark red]) and Roche color card (range: 11 [light orange] to 18 [dark red]) (Hoffmann-La Roche, Basel, Switzerland) (Figure 3). Images of fillets were captured on the same day the sensory and the instrumental evaluation of color were performed, but they were processed later.

Image acquisition

The images of fillets for color assessments were captured using a computer vision system (Figure 1) for a digital color camera (Nikon Coolpix5000, Nikon, Tokyo, Japan) at the resolution of 1600 × 1200 pixels. Images were acquired in the JPEG format and processing was carried out in the captured images (still). However, commercial industrial full frame digital cameras with comparable resolution are available at near real-time speeds (Pacer Components PLC, Berkshire, England). The use of a line-scan color camera is most likely preferable in an industrial setting, due to their high speed and the fact the fish in most cases are transported on conveyor belts. The white balance of the camera was set using the camera automatic white balance based on a white plate covering the entire field of view of the camera. Two different illumination setups were used during the image acquisition. The first setup, for color evaluation of fillet Group I, used 2 parallel halogen lamps with color temperature 2900 K and 300 W each (Figure 4). The lamps were placed 30 cm below the fillet, whereas the reflecting white cardboard plates were set at an angle of 45°. Reflection plates were used to provide with diffuse illumination in order to avoid specular reflections from the fillet and to improve the quality of the captured images. The images were acquired freehand in a 90° angle, 60 cm above the fillet. The 2nd setup, for evaluation of fillet Group II, used 4 lamps (2900K, 15W, 135 mA) as suggested by Papadakis and Abdul-Malek (2000) (Figure 5). In this setup, the lamps were positioned in a 45° angle and 40 cm above the fillet, whereas the camera was fixed to a bar, perpendicular to the plane where the fillets were located.

Image segmentation and enhancement

Color analysis and classification of fillets according to Roche cards by computer vision were performed in red, green, and blue (RGB)

Figure 2 – The computer vision color data were compared with Roche *Salmo*Fan™ and Roche Color Card readings and L^*, a^*, and b^* values in locations 1 to 5. Numbers on the fish are the locations where the measurements were made.

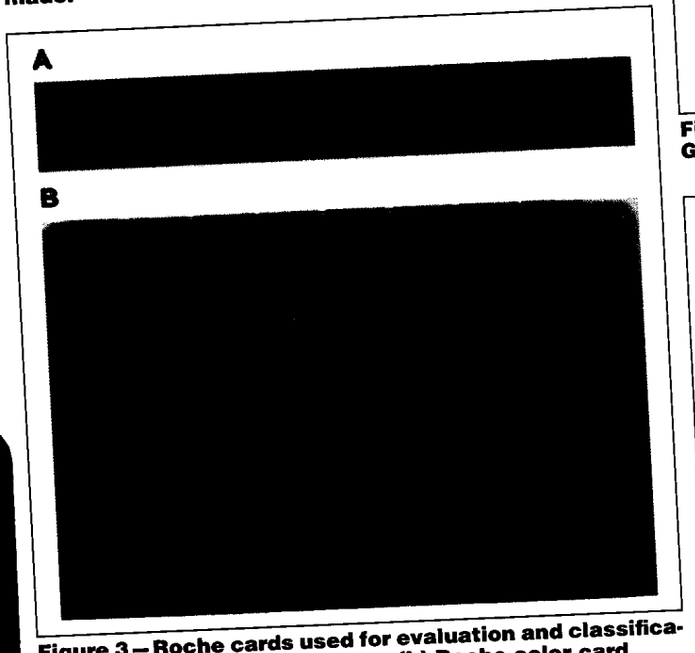

Figure 3 – Roche cards used for evaluation and classification: (a) Roche *Salmo*Fan ruler, (b) Roche color card

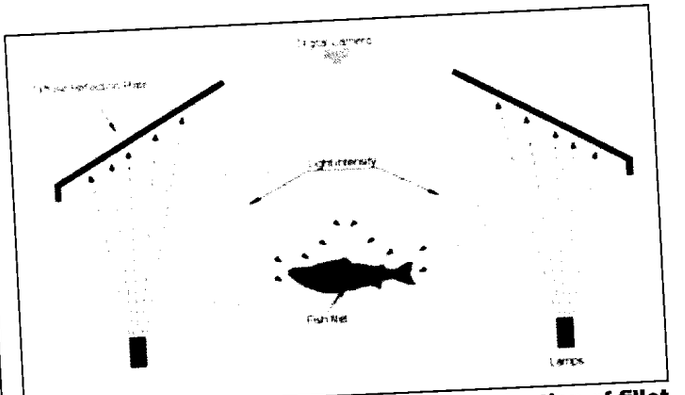

Figure 4 – Experimental setup for the illumination of fillet Group I

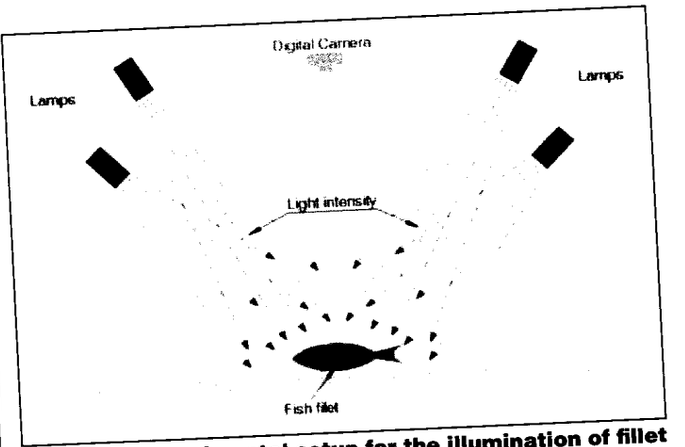

Figure 5 – Experimental setup for the illumination of fillet Group II

and CIE $L^*a^*b^*$ color space. The algorithm for classification of the fillets was developed within the Matlab 6.5 Development Environment (Mathworks, Mass., U.S.A.) using the Image Processing Toolbox 3.2. The sequence of the classification algorithm is depicted in Figure 6. After image acquisition, the fillet could be isolated from background either in Matlab or even simpler in Adobe Photoshop (Adobe, San Jose, Calif., U.S.A.), in order to be viewed as a single region of interest for further analysis. For the purpose of this work, the segmentation was optional, but in an online application the segmentation of fillets from the background would be necessary for the purpose of color matching. Then, the segmented image was converted to a true color RGB image, isolating the fillet from the image background (not of interest for further analysis). The image enhancement consisted of filtering the fillet images from high frequent components and noise. From the color scores of the Roche *Salmo*Fan™ ruler and Roche color card, we generated a look-up table by integrating the color of every color rectangle and finding its mean value. For the color evaluation of the fillets according to the Roche *Salmo*Fan ruler, we used all color scores (20 to 34), while for the evaluation according to the Roche color card, we used the color scores designated with numbers from 11 to 18 (Skrede and others 1990).

Normalized RGB and look-up table generation

In the look-up table, the information for each color score of the Roche ruler was memorized in form of means of normalized red (R), green (G), and blue (B) values. The normalization of RGB values was done to remove the device dependency toward the RGB color space and to remove the brightness. The normalized values were calculated from these expressions:

$$r = \frac{R}{R+G+B} \tag{2}$$

$$g = \frac{G}{R+G+B} \tag{3}$$

$$b = \frac{B}{R+G+B} \tag{4}$$

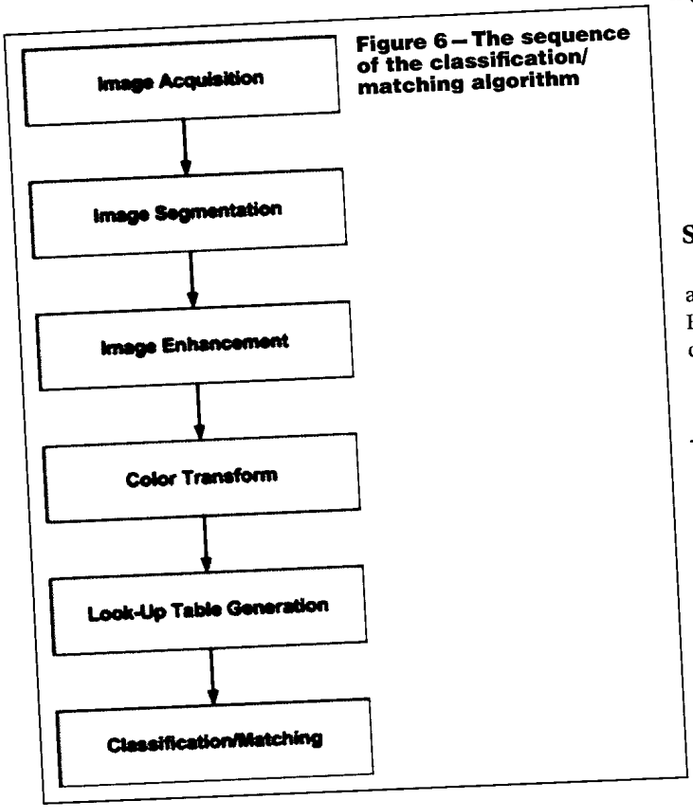

Figure 6—The sequence of the classification/ matching algorithm

Color feature extraction and classification

From the mean r_{li}, g_{li}, r_{ci}, and g_{ci} values, the algorithm created 15 color pairs (r_{li}, g_{li}), one for each value of the Roche *Salmo*Fan ruler, and 8 color pairs (r_{ci}, g_{ci}) for the Roche color card. For a normalized values of red, green, and blue (RGB), the relationship $r + g + b = 1$ holds (Panigrahi and Gunasekaran 2001), and hence the value b is not taken into consideration, because it can always be calculated by simply taking $b = 1 - (r + g)$. After the retrieval of mean values for R and G for each Roche color score, the algorithm proceeded with the calculation of the mean red and green values for the regions of interest in the fillet (Figure 2). There were 5 regions of interest the algorithm dealt with. Each region of interest was chosen simply by clicking with a mouse on the region of interest in the fillet image for classification according to Roche ruler. For each fillet, the algorithm calculated 5 pairs of mean values for red and green, each pair corresponding to the chosen region of interest, and compared these with the matching pairs

$$m_j = (r_j, g_j),\ j = 1, \ldots 15 \tag{5}$$

from the Roche *Salmo*Fan ruler. Geometrically, pairs r_{li},g_{li} lie in the plane r_lOg_l, whereas pairs r_{ci}, g_{ci} lie in the plane r_cOg_c. Determination of the matching Roche scores of the selected regions of interest was done according to the nearest neighbor principle (Theodoridis and Koutroumbas 2003). This means that the region of interest was assigned the color of its nearest neighbor. Calculation of distances for the nearest neighbor rule was done by calculating the Euclidian distance between the fillet point $\overline{p_i}$ in red, green, and blue (RGB) space and Roche color vector m_j (Gonzales and others 2004) which is given by

$$D_E(\bar{p}, m) = \|p - m\| = \left[(p_R - m_R)^2 + (p_G - m_G)^2\right]^{1/2} \tag{6}$$

The estimated Roche score of the fillet point $\bar{p}_i$ is computed by

$$R(\bar{p}_i) = 19 + \arg \min_{j=1,\ldots 15} D_E(\bar{p}_i, m_j) \tag{7}$$

Statistics

Mean, standard deviation was calculated and analysis of variance (ANOVA) was performed using Minitab 14.1 (Minitab Inc., Pine Hall, U.S.A.) statistical software. A significance level of $P < 0.05$ was chosen.

Results and Discussion

A major finding regarding the fillet color (Figure 2) was that, for both groups, no significant differences ($P > 0.05$; Table 2) in the color values according to Roche card were found between the computer vision method and the traditional method of sensory evaluation of color by human inspectors. From Table 1, it is seen that the color discrimination did not differ much from the sensory evaluation method and the computer vision method. By looking at the means and the standard deviations (Table 1) between sensory evaluation and computer vision method of color measurement according to the Roche cards, it was noted that there was no significant difference between them. This was evident for both groups. As is seen in Table 1, computer vision evaluation gave higher values in Roche scores for 1 unit than the sensory evaluation method for 2 of overall 5 fillet locations. Statistical analysis (Table 2) for both groups of

Table 1 – Comparison of color values in different 5 locations (Figure 2) on Atlantic salmon fillets as determined by computer vision and the Roche *Salmo*Fan ruler

Method	Fillet color values				
	1	2	3	4	5
Group I*					
Roche SalmoFan-visual	23[a]	23[a]	20[a]	22[a]	21[a]
Computer vision	22[a]	20[a]	21[a]	21[a]	20[a]
Group I					
L^* (Minolta-M)	40 ± 1	39 ± 2	38 ± 1	45 ± 3	45 ± 2.5
a^* (M)	11 ± 1	11 ± 0.5	12 ± 1	12 ± 2	12 ± 1
b^* (M)	11 ± 1	11 ± 1	12 ± 1.5	13 ± 3	15 ± 2
L^*(computer vision-CV)	62 ± 1	63 ± 0.5	62 ± 2	64 ± 0.5	64 ± 1
a^* (CV)	34 ± 3	33 ± 3	38 ± 2	27 ± 3	28 ± 2
b^* (CV)	58 ± 3	59 ± 3	61 ± 2	54 ± 3	54 ± 3
Roche SalmoFan-visual	28 ± 1	28.5 ± 1	29 ± 1	22 ± 1	23 ± 1
Computer vision	29 ± 1	29 ± 1	30 ± 1	23 ± 1	23 ± 1
Group II[†]					
L^* (Minolta-M)	40.25 ± 2.4	40 ± 2	38 ± 1.3	51 ± 3	51 ± 6
a^* (M)	11.8 ± 1	12 ± 1	11.5 ± 1	15 ± 1.5	13 ± 1.3
b^* (M)	12 ± 2	12.8 ± 1	11.5 ± 1.7	17.5 ± 2.5	15 ± 2
L^* (CV)	64.3 ± 0.5	64 ± 0.5	64 ± 1	65.5 ± 0.5	66 ± 0.5
a^* (CV)	26 ± 3	28 ± 2.5	28 ± 5	18 ± 3	17 ± 1.5
b^* (CV)	59 ± 6	63 ± 3	55 ± 7	50 ± 7	50 ± 4.5
Roche SalmoFan-visual	27 ± 1	28 ± 1	27 ± 2	24 ± 2	23 ± 2
Computer vision	28 ± 1	28 ± 1	28 ± 2	23 ± 2	23 ± 2

[a]Sexually mature fish (n = 1).

fillets included all fillets and their color scores (consequently all the means of color values in Table 1) measured by the sensory evaluation method and the computer vision method. This analysis showed that there was no significant difference between the sensory evaluation method and computer vision method.

An immediate implication of these results is that the computer vision method is not different from the traditional sensory evaluation of fillet color. The advantages of using computer vision in automating the operation of color sorting of salmon fillets, as reported in (Irudayaraj and Gunasekaran 2001), are the long-term consistency and objectivity in color assessment. This is because in computer vision, there is no eye fatigue or lack of color memory, and illumination conditions are uniform (Irudayaraj and Gunasekaran 2001). In addition, automation of this operation can bring a reduction in labor costs and production costs. Automation can remove the need for operator facilities, lighting, heating, clothing, and washing facilities (Purnell 1998). An important ability of computer vision method is that once the image of fillet is captured, one can measure the color of the entire fillet (the mean color value) or one can measure the color of a specific region of interest, as in locations (1 to 5) in Figure 2.

The color scores were significantly different from 1 point to another point of assessment ($P = 0.000$) on the fillet for both groups of fillets no matter which method for color evaluation was used (color of location 1 is different from the color of location 5). This was because locations in the white muscle (1 to 3), where we measured the color, were redder than locations (4 to 5) in the belly flap. In Table 1, it is shown that L^* values for the white muscle locations (1 to 3) were lower from those of belly flap locations (4 to 5), which means that the belly flap locations are brighter. The same conclusion is drawn by looking at the values generated by the computer vision method and sensory evaluation according to the Roche card standard. Both of these methods gave higher (redder) Roche color card scores for the white muscle locations (1 to 3) than for those of belly flap (4 to 5).

The significance level (0.997 > 0.119) for method comparison was higher for the 1st group (Method*Point in Table 2) than for the 2nd. In this table are shown the difference between sensory evaluation method and computer vision method (Method in Table 2), the difference between locations of assessment for both methods (Point in Table 2), and the difference between the methods taking all points into the account (Method*Point in Table 2). The higher significance level for the 1st group may be due to different illumination setups used for the image acquisition but also due to the different group sizes. By analyzing L^* values for both groups, it was noted that the 1st group was slightly darker in the muscle flesh (Table 1). By looking at the L^* values generated by both the chromameter and the computer vision algorithm, it is seen that the 1st group appeared slightly darker than the 2nd one. This was also confirmed by the Roche color card scores obtained from the sensory evaluation and the computer vision algorithm. The means of color assessments according to the Roche color card for both of these methods were higher for the 1st group.

Computer vision values for the color scores of fillets generated by the algorithm were consistent, because the algorithm gave the same values under the given illumination conditions, and was invariant to illumination, provided that the illumination was the same for all fillets, which were used in the classification. On the other hand, human ability to distinguish color tends to be subjective. This can make the same Roche scores be interpreted differently, depending on light conditions, that is, whether human inspectors were performing classification in the daylight conditions or in the artificial illumination conditions. Provided that illumination is controlled, for example, in a light box, the assessment of fillet color with computer vision algorithm would be consistent and stable.

Table 2 – Analysis of variance (ANOVA) for the computer vision method of evaluation and the method used by human inspectors

	P value
Group I	0.715
Method	0.000
Point	0.997
Method* Point	
Group II	0.189
Method	0.000
Point	0.119
Method* Point	

When it comes to the Minolta chromameter measurements, the CIELab values generated by the Minolta chromameter and those generated by the computer vision algorithm showed large deviations in mean value (Table 1). For instance, the mean of the computer generated L^* value for a certain location of color assessment was on average 23 units higher than the value measured with chromameter. This deviation is within the standard range reported earlier in the Kim and others (2005), and it is due to the brighter illumination used by the computer vision setup. The Minolta chromameter uses a pulse of xenon light to illuminate the examination area, which is 8 mm in diameter and measures the reflected light from the flesh.

This made CIELab values generated by the Minolta chromameter not comparable with the CIELab values generated from the computer vision algorithm, as reported in Kim and others (2005). The CIELab values by algorithm were obtained by converting the normalized RGB values into the CIELab color space. However, the converted color values may differ considerably from the standard CIELab values taken with chromameter and, therefore, would not allow the comparison of values between those generated by algorithm and those generated by chromameter (Kim and others 2005).

Conclusions

The results have demonstrated the ability of the method based on computer vision to classify fillets according to color. This method was a fast, nondestructive, and contact-free evaluation and was not significantly different from the traditional method of evaluating the color by human vision. The results have demonstrated that the computer vision-based method of evaluating color was just as good as the traditional one. The better side of the computer vision method is that this method is faster, robust, and consistent. Since human operators are a factor in product contamination, the costs of preserving hygiene with the large numbers of staff present in a fish processing plant increase the overall production cost. The use of computer vision would result in a decrease of product contamination. With the automation of fish processing, there would also be less need for lighting and heating of the production premises and automation would allow processing in environments beneficial to quality of fish products, for example, sustained low temperatures. Time savings would also be considerable. A computer vision system is designed to process a minimum of 1 fillet per second, while human inspectors use longer time when using either a sensory or instrumental method because they are susceptible to fatigue and because of the involved labor. And finally, the fish processing plants would save $1 per kilogram in labor costs. These are the estimated labor cost savings for the Norwegian fish processing industry. When it comes to implementation of the computer vision system in the future, it is preferred to use controlled illumination conditions for the purpose of classification of fillets, for example, by using a light box with a uniform illumination. Results showed that computer vision-based classification can be successfully used to replace human inspectors in the color assessment of salmon fillets.

Acknowledgments

The project was funded by the Research Council of Norway (NFR project No. 145634/140–"Efficient and economic sustainable fish processing industry").

References

Abdullah MZ, Aziz SA, Mohamed AMD. 2000. Quality inspection of bakery products using a color-based machine vision system. J Food Quality 23(1):39–50.
Anderson S. 2000. Salmon color and the consumer. Proc. Int. Inst. of Fisheries Economics and Trade (IIFET) Conf.; Corvallis, Oregon, USA.
Arnarson H, Bengoetxea K, Pau LF. 1988. Vision applications in the fishing and fish product industries. Int J Pattern Recognition Artificial Intelligence 2:657–71.
Barnham C, Baxter A. 1998. Condition factor K for salmonid fish. Dept. of Primary Industries. State of Victoria. Available from: http://www.ourwater.vic.gov.au/dpi. Date accessed: Aug 29, 2006.
Brosnan T, Sun DW. 2004. Improving quality inspection in food products by computer vision-a review. J Food Technology 61(2–3): 3–16.
CIE (1976) 18th Session, London, UK., Sept. 1975. CIE Publication 36, Paris, France.
Davidson VJ, Ryks J, Chu T. 2001. Fuzzy models to predict consumer ratings for biscuits based on digital features. IEEE Trans Fuzzy Syst 9(1):62–7.
Duda RO, Hart PE, Stork DG. 2001. Pattern classification. New York: John Wiley & Sons. p 11.
Fulton T. 1902. Rate of growth of seas fishes. Sci Invest Fish Div Scot Rept 20.
Gonzales RC, Woods RE, Eddins SL. 2004. Digital image processing using Matlab. Upper Saddle River, N.J.: Pearson Prentice Hall. p 237.
Irudayaraj J, Gunasekaran S. 2001. Optical methods: visible, NIR, and FTIR spectroscopy. In: Gunasekaran S, editor. Nondestructive food evaluation techniques to analyze properties and quality. New York: Marcel Dekker. p 1–2.
Kim Ch-S, Kim MK, Jung B, Choi B, Verkrysse W, Jeong M-Y, Nelson JS. 2005. Determination of an optimized conversion matrix for device independent skin color image analysis. Lasers Surg Med 37(2):138–43.
Lin M, Cavinato MG, Mayes DM, Smiley S, Huang Y, Al-Holy M, Rasco BA. 2003. Bruise detection in Pacific Pink salmon *(Oncorhynchus gorbuscha)* by visible and short-wavelength near-infrared (SW-NIR) spectroscopy (600-1100 nm). J Agric Food Chem 51(22):6404–8.
Mery D, Pedreschi F. 2004. Segmentation of color food images using a robust algorithm. J Food Eng 66(3):353–60
Misimi E, Mathiassen JR, Erikson U, Skavhaug A. 2006. Computer vision based sorting of Atlantic salmon *(Salmo salar)* according to shape and size. Proceedings of VISAPP Intl. Conference on Computer Vision Theory and Applications; 2006 February 25–28; Setubal, Portugal. p 265–70.
NBS 10-01. 1999. Quality grading of farmed salmon. Bergen: Norwegian industry standard for fish.
NS 9402. 1994. Atlantic salmon, measurement of color and fat. Oslo: Norwegian Standards Assn.
Osland E. 2001. Rainbow trout of SalmoBreed Production. SalmoBreed, Norway. Available from: http://www.salmobreed.no/WordDoc/Sheetnr4.Porductionoftrout.pdf?AnnID/45#search/%22the%20japanese%20SalmoBreed%22. Date accessed: 09/05/2006.
Ostvik S, Jansson S. 2004. Comparison of today's production system in Norway with the production in Poland and China as countries with low production costs. In: Efficient and sustainable fish processing industry. Trondheim: SINTEF Fisheries and Aquaculture.
Panigrahi S, Gunasekaran S. 2001. Computer vision. In: Gunasekaran S, editor. Nondestructive food evaluation techniques to analyze properties and quality. New York: Marcel Dekker. p 39–92.
Papadakis SE, Abdul-Malek S. 2000. A versatile and inexpensive technique for measuring color of foods. J Food Technol 54:12.
Pau LF, Olafsson R. 1991. Fish quality control by computer vision. New York: Marcel Dekker. p 23–38.
Purnell G. 1998. Robotic equipment in the meat industry. Meat Sci 49(1):S297–307.
Schmidt PJ, Cuthbert RM. 1969. Color sorting of raw salmon. Food Technol 23:98–100.
Skrede G, Risvik E, Huber M, Enersen G, Blumlein L. 1990. Developing a color card for raw flesh of astaxanthin-fed salmon. J Food Sci 55(2):361–363.
Strachan NJC. 1993. Recognition of fish species by color and shape. Image Vis Comput 11:2–10.
Strachan NJC, Murray CK. 1991. Image analysis in the fish and food industries. In: Pau LF, Olafsson R, editors. Fish quality control by computer vision. New York: Marcel Dekker. p 209–23.
Theodoridis S, Koutroumbas K. 2003. Pattern recognition. San Diego, Calif.: Academic Press. p 44–6.